frontiers | Frontiers in Earth Science

ORIGINAL RESEARCH
published: 04 May 2022
doi: 10.3389/feart.2022.876196

Particle Size and Internal Structure of Deformed Coal: Microstructure and Adsorption/Desorption Characteristics of CO_2 and CH_4

Xiaoshi Li[1,2,3], Yiwen Ju[1], Yu Song[4], Zhifeng Yan[1,5] and Qiangguang Li[1,6]*

[1]Key Laboratory of Computational Geodynamics, College of Earth and Planetary Sciences, University of Chinese Academy of Sciences, Beijing, China, [2]Institute of Geomechanics, Chinese Academy of Geological Sciences, Beijing, China, [3]Key Laboratory of Paleomagnetism and Tectonic Reconstruction, Ministry of Natural Resources, Beijing, China, [4]Key Laboratory of Coalbed Methane Resource & Reservoir Formation Process, Ministry of Education, School of Resources & Earth Science China University of Mining and Technology, Xuzhou, China, [5]School of Earth Science and Engineering, Hebei University of Engineering, Handan, China, [6]Key Laboratory of Karst Georesources and Environment, Ministry of Education, College of Resource and Environmental Engineering, Guizhou University, Guiyang, China

Structural deformation has a very important effect on the particle size and adsorption/desorption properties of coal, which is widely distributed in China, but there are few studies in this area. The effects of particle size and internal structure on the pores and adsorption properties of deformed coal were studied, and the influence of structural deformation was analyzed. Eight undeformed and deformed coal samples were progressively crushed from 0.12 to 0.15 mm (100–120 mesh), 0.18–0.25 mm (60–80 mesh), and 0.42–0.84 mm (20–40 mesh), and subsequently, adsorption/desorption characteristics of CO_2 and CH_4 and pore structure analyses were performed on all the grain size fractions. The coal size fraction has a slightly smaller influence on CO_2 adsorption than on CH_4 adsorption. Deformation can promote gas desorption, which increases as the deformation increases. Moreover, deformation can reduce the effect of granularity and internal structure on gas adsorption capacities. The 60–80 mesh is suggested to be the optimal size for deformed coal to achieve the ideal adsorption/desorption effect without eliminating the influence of structural deformation. However, below 100–120 mesh is recommended to reduce the impact of structural deformation on data processing and analysis when the sample contains both deformed and undeformed coals.

Keywords: deformed coal, particle size, internal structure, microstructure, adsorption/desorption characteristics

OPEN ACCESS

Edited by:
Candan Gokceoglu,
Hacettepe University, Turkey

Reviewed by:
Hasril Hasini,
Universiti Tenaga Nasional, Malaysia
Hongjian Zhu,
Yanshan University, China

***Correspondence:**
Yiwen Ju
juyw03@163.com

Specialty section:
This article was submitted to Economic Geology, a section of the journal Frontiers in Earth Science

Received: *15 February 2022*
Accepted: *19 April 2022*
Published: *04 May 2022*

Citation:
Li X, Ju Y, Song Y, Yan Z and Li Q (2022) Particle Size and Internal Structure of Deformed Coal: Microstructure and Adsorption/Desorption Characteristics of CO_2 and CH_4. Front. Earth Sci. 10:876196. doi: 10.3389/feart.2022.876196

1 INTRODUCTION

Coal is a complex polymeric material with a complex pore structure. Most scholars consider that coalbed methane (CBM) in coal seams mainly exists in an adsorbed state (Cao and Zhang, 2003a, Cao et al., 2003b; Busch et al., 2003; Ju and Li, 2009). Therefore, the coal adsorption property is an important index of the release of coal seam gas. Studies on coal adsorb ability have been extremely significant in the development of CBM and for predictions of the gas content (Gayer and Harris, 1996; Cui et al., 2005; Islam and Hayashi, 2008). The main factors that are currently considered to affect coal adsorption are the composition, mineral content, temperature, pressure, metamorphic degree, and structural deformation (Crosdale and Beamish, 1993; Busch et al., 2003; Qu, 2011; Zou

and Rezaee, 2016; Li et al., 2019a; Li et al., 2019b). Many scholars have reported that the coal adsorption capacity increases with the metamorphic degree for $R_{o,\,max} < 4.0\%$ (Yao and Liu, 2007; Jiang et al., 2010). Zhong et al. found that the coal adsorption capacity for methane decreased as the temperature increased, and this change was more marked at higher pressures (Zhong et al., 2002). Hou et al. characterized the pore structure of coals with different particle sizes that formed under structural deformation and reported that structural deformation increases the abundance of accessible mesopores and causes micropore collapse Hou et al. (2017). Pan et al. studied the effects of temperature and pressure on the adsorption capacity of deformed coal, which was found to decrease as the temperature increased and was significantly higher for ductile deformed coal than for weak brittle deformed coal Pan et al. (2012). Qu et al. found that the adsorption capacity of deformed coal increased significantly with deformation because of the deformation-induced formation of a complex pore system Qu, (2011); (Zhu et al., 2018, 2020).

Many studies have been conducted on the effect of sample size on the adsorption/desorption properties of coal (Zhang et al., 2009; Sun et al., 2012; Han et al., 2013; Jia et al., 2013; Marcin et al., 2016; Mastalerz et al., 2017). For example, through CH_4 adsorption experiments with different particle sizes, Sun et al. reported that the smaller the particle size is, the larger the specific surface area and adsorption capacity (Zhang et al., 2009); Sun et al. (2012). Jia et al. conducted CH_4 adsorption/desorption experiments on coal with different particle sizes (0.2–0-0.5 mm, 0.5–1-1 and 1.3 mm) and believed that within a certain time range, the particle size of coal is inversely proportional to the total gas desorption Jia et al. (2013). However, one of the most common problems associated with adsorption/desorption property studies on coal samples is the particle size of samples chosen for the experiments. In the vast majority of laboratory sorption experiments, the samples are crushed and sieved to a given fraction before the experiment starts, which influences the experimental data and analysis. Regarding coals, the fraction that passed through a 60 mesh (0.25–0.2 mm) sieve has been preferred, but other analytical size fractions have also been used, including but not limited to 4 mesh (<4.78 mm), 7 mesh (<2.83 mm) (Furmann et al., 2016), 16 mesh (<1.18 mm) (Swanson et al., 2015), 100 mesh (<0.125 mm) and 200 mesh (<0.074 mm) (Cao et al., 2015; Wang and Ju, 2015; Marcin et al., 2016). Mastalerz et al. studied N_2 and CO_2 adsorption in coal and shale for different particle sizes [chunks (~7 mm) to 4 mesh (<4.78 mm), 7 mesh (<2.83 mm), 18 mesh (<1 mm), 30 mesh (0.595 mm), 60 mesh (<0.250 mm), 200 mesh (<0.074 mm), and 230 mesh (<0.063 mm)] and determined that the most suitable particle sizes for adsorption analysis were the 60-mesh fraction for coal and 200 mesh fractions for shales (Mastalerz et al., 2017).

Complex tectonic movement has produced widely developed deformed coals in most coal-bearing basins in China (Cao and Zhang, 2003a, Cao et al., 2003b; Ju et al., 2005a). Deformation crushes coal and affects its pore structure and macromolecular structure, which in turn affects adsorption and desorption in this material (Domazetis and Raoarun, 2008; Chen et al., 2011; Mathews et al., 2011; Castro and Lobodin, 2012; Cai et al., 2013; Li et al., 2014). However, relatively few studies have been performed on the adsorption performance of deformed coal of different particle sizes. When the adsorption performance and pore structure of deformed coal are studied, the selection of sample size fractions will affect the results. If the coal samples collected contain deformed coal and undeformed coal, then the sample size should be selected to be the most appropriate during the experiment because the influence of structural deformation on the particle size and pore structure of coal cannot be ignored. Therefore, in this paper, we collected samples of brittle and ductile deformed coal to perform a comparative analysis using undeformed coal as a reference. We conducted experiments on the isothermal adsorption of CH_4 and CO_2 in coal of different particle sizes to investigate the effect of deformation and particle size and internal structure on the coal adsorption performance. The suitable experimental size range of deformed coal is also discussed.

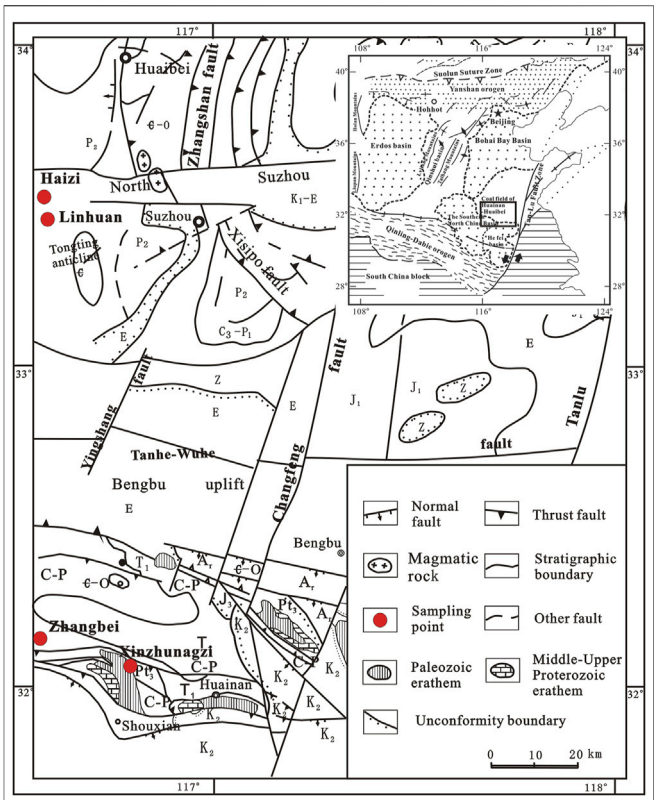

FIGURE 1 | The samples distribution plot (after Ju et al., 2005a; Li et al., 2012).

2 SAMPLES AND METHODS

2.1 Geological Settings and Samples

All coal samples were collected from the Permo-Carboniferous coalbed in the Huainan-Huaibei coalfield, which was strongly affected by Mesozoic tectonic deformation (**Figure 1**). The coal seams are distributed mainly in the graben part, especially in the

TABLE 1 | Coal sample characteristics.

Deformation series		Sample No	Deformation degree	Characteristics of macroscopic hand-formed specimens
Undeformed coal		P01	/	The undeformed can be observed. The coal is hard and difficult to separate by hand
		P02	/	
Deformed coal	Brittle deformation	B01	Weak	Brittle deformed coal usually has multidirectional or unidirectional fractures, and the undeformed can be observed. The coal is hard and not easily broken
		B02	Weak	
		B03	Strong	The undeformed is damaged, and the coalbedding has almost disappeared. The coal has subangular or subround particles and develops small fractures in different directions. The coal has a low strength and can be powderized by hand
	Ductile deformation	D0s1	Weak	Wrinkle and mylonitic structure can be observed in the coal. The coal petrographic composition is not easily discriminated. The coal is soft and can be easily pinched into fragments
		D02	Weak	
		D03	Strong	The coal petrographic composition is strongly wrinkled and forms irregular crumb structures that cannot be discriminated. The coal can be turned into fine grains or powder by hand

syncline part. A series of multiple synclines and anticlines are distributed in this area with a NNW-NE strike. The structural deformation remarkably destroyed the structure of coal seams, resulting in the widespread development of brittle and ductile deformed coal in this area (Ju et al., 2005a; Li et al., 2012).

Deformed coal is formed under one or more periods of tectonic stress. The original structure is deformed (crushed, folded, etc.) or undergoes superimposed damage in different degrees of stress, and even the internal chemical composition and structure are changed (Ju et al., 2004). Deformed coal can be divided into three types, namely, brittle deformation, ductile deformation and brittle-ductile transition, according to the structural composition and mechanical properties (Hou et al., 1995; Guo, 2001; Jiang and Ju, 2004; Ju et al., 2004, 2005a, 2009). The brittle deformation series shows the development of one or more groups of joints or fractures. Strong brittle deformation leads to dislocation of the coal particles cut by joints and cracks and is even rounded to form a clastic structure. A ductile deformation series is formed under certain strata temperature and pressure conditions, and the coal seam is ductile deformed under extrusion or shear stress, forming various ductile structures such as folds and flowing deformation (Cao et al., 2003b; Jiang and Ju, 2004; Ju et al., 2004, 2005a, 2009; Wang et al., 2009; Qu et al., 2012). Brittle-ductile deformation is a transition type between brittle deformation and ductile deformation.

Eight coal samples in this paper were evaluated according to the above classification. Six deformed coal samples were collected from the Xinzhuangzi, Linhuan and Haizi coal mines. Additionally, to serve as a reference for the deformed coals, we obtained two undeformed coal samples from the Zhangbei coal mine that were almost unaffected by structural deformation (**Figure 1**). The characteristics of coal hand specimens with different deformation degrees are quite obvious and are described in detail in **Table 1**. All the samples were labeled by the coal type: the undeformed coal samples were labeled P01 and P02; the brittle deformed coal samples were labeled B01, B02, and B03; and the ductile deformed coal samples were labeled D01, D02, and D03 (**Table 1**).

2.2 Experimental Methods

The metamorphic grade, proximate analysis and component composition after purification of all coal samples were analyzed before the experiment (**Table 2**). The table shows that the coal samples are mainly of low or medium ash, with an ash yield between 8.93 and 44.31%, volatile matter (*V*) content ranging from 10.04 to 34.99%, moisture content varying from 0.79 to 1.84%, and fixed carbon content ranging from 36.35 to 79.05%.

According to the different specific gravity values of each component, the vitrinite of the coal sample was separated and purified by hand picking and then density gradient centrifugation (Dyrkacz and Horwitz, 1982; Gilfillan et al., 1999; Ju et al., 2005b; Wang et al., 2005) to reduce the influence of coal components on the adsorption/desorption performance. Before the adsorption/desorption test, all deformed coal samples were crushed and sieved to 20–40 mesh and then treated with vitrinite centrifugation based on hand-picked vitrinite. We used benzene and carbon tetrachloride (CCl_4), which are volatile and have no effect on the coal structure, to refine the amount of vitrinite up to 80%–99% (Li et al., 2010, 2014). Please refer to previous articles for specific methods (Dyrkacz and Horwitz, 1982; Ju et al., 2005b; Li et al., 2010, 2014).

Vitrinite accounts for between 81.90 and 96.30% of the samples, the inertinite content ranges from 1.60 to 12.52% and almost no liptinite is present. The mineral content ranges from 0.19 to 2.56%. As seen from **Table 2**, except for sample P01 (81.9%), the vitrinite content of all the other samples is above 85%, and the mineral content is below 3%. Therefore, these processes will increase the vitrinite content and minimize the effects of maceral composition on the pore structure.

2.2.1 Scanning Electron Microscopy Observation

Scanning electron microscopy (SEM) can help us better understand the microstructure on small particle coal surfaces and analyze the fracture forms and internal structure of coal. SEM measurements were performed at Henan Polytechnic University. Coal samples collected were observed by SEM (JSM 6390/LV) with an acceleration voltage of 0.5–30 kV and 150–3000× magnification.

2.2.2 Adsorption Method

Before the adsorption experiments were performed, the eight samples were prepared by crushing and sieving the coal into three

TABLE 2 | Properties of coal samples.

Sample No	$R_{o,\ max}$ (%)	Proximate analysis (air-dried basis, wt%)				Maceral analysis after purification (%)			
		M	*A*	*V*	*FC*	Vitrinite	Inertinite	Liptinite	Mineral
P01	0.97	1.70	13.82	34.99	49.50	81.90	10.09	5.43	2.57
P02	1.29	0.93	44.31	18.42	36.35	90.24	8.79	/	0.97
B01	1.08	1.33	8.93	28.29	61.45	95.29	2.52	/	2.19
B02	1.11	1.84	10.41	27.64	60.12	86.09	12.52	/	1.39
B03	1.31	0.83	9.83	26.60	62.75	92.34	4.73	0.37	2.56
D01	1.56	0.79	11.54	25.33	62.35	96.10	1.60	0.40	1.90
D02	1.63	0.93	15.57	21.57	61.94	96.30	1.97	/	1.72
D03	1.93	1.64	9.27	10.04	79.05	89.83	9.22	0.75	0.19

M *is the moisture content,* A *is the ash content,* V *is the volatile matter content, and* FC *is the fixed carbon.*

size ranges [0.12–0.15 mm (100–120 mesh), 0.18–0.25 mm (60–80 mesh), and 0.42–0.84 mm (20–40 mesh)], followed by outgassing at 298 K for 24 h in a vacuum oven. This procedure was used to completely remove any adsorbed gas from the coal matrix. The coal samples were aerated with high-purity CH_4 (99.9%) and high-purity CO_2 (99.9%) under humidity/temperature balance conditions (0.93%/30°C). Isothermal adsorption experiments were performed using an IS-300 automatic isothermal adsorption instrument. The pressure ranges used to measure gas adsorption were 0.5–12 MPa for CH_4 and 0.5–5 MPa for CO_2. The adsorption capacity was determined at various pressures, and the adsorption equilibrium time was 24 h.

2.2.3 Calculation of Langmuir Isotherms

Adsorb ability is a natural property of porous materials, including coal. The solid surface of coal and a gas form a system, and the phenomenon of gas components accumulating at the two-phase interface is called adsorption. The return of adsorbed gas molecules to the gas phase is called desorption. Coal adsorption is currently considered to involve mostly physical adsorption, as represented by the Langmuir adsorption model (Laxminarayana and Crosdale, 1999; Yu et al., 2004; Moore, 2012).

The Langmuir model is often referred to as monolayer adsorption theory, where the governing formula is simple and practical and has been widely used to describe gas adsorption in coal and other adsorbents. Most of the instruments used to measure isothermal adsorption in coal are designed in accordance with this theory. The Langmuir parametric formula is given as follows:

$$V = \frac{V_L P}{P_L + P} \tag{1}$$

where P is the pressure of sorbate gas (MPa); V is the adsorption capacity under pressure P (m^3/t); V_L is the Langmuir volume (m^3/t); and P_L is the Langmuir pressure (MPa).

Defining A = $1/V_L$ and B=P_L/V_L, **formula (1)** can be written in terms of A, which is a function of P/V and P:

$$P/V = P/V_L + P_L/V_L \text{ or } P/V = AP + B \tag{2}$$

Formula (2) can be used to create scatter plots of the measured pressure and adsorption data at different equilibrium pressures with P as the abscissa and P/V as the ordinate. The regression formula and correlation coefficient of these scatter plots can be obtained by using the least squares method, where the slope of the straight line is A and the intercept is B. In this study, the slope and intercept were used to calculate the Langmuir volume and the Langmuir pressure as follows:

$$V_L = 1/A, P_L = B/A \text{ or } P_L = V_L B \tag{3}$$

The isothermal adsorption/desorption curve was plotted using the adsorption capacity and pressure for different equilibrium pressures.

3 RESULTS

3.1 Particle Characteristics of Coal From SEM Imaging

The grain fragments of undeformed coal, brittle deformed coal and ductile deformed coal were observed by SEM (**Figure 2**). The undeformed coal (**Figures 2A–D**) grains are intact, the bedding is well preserved, and fractures are hardly observed. The pore distribution can be seen on the particle surface (red circle). In the brittle deformed coal (**Figures 2E–J**), fractures are developed, and particles are layered (**Figures 2E–H**). Smaller particles are sometimes observed agglomerating in fractures. Complete particles can be partially cut or fully penetrated by fractures, but the particles are still connected without further crushing. Due to fracture development, pores inside the particle are connected with surface pores (**Figures 2I,J**). Wrinkles can also be seen on the particles of the ductile deformed coal, and flake particles can sometimes be observed (**Figures 2K–P**). Most of the ductile deformed coal particles are formed by agglomeration of small particles (**Figures 2K–N**), with a large number of pores, fractures and high connectivity, indicating that ductile deformation has caused the granulation of coal and destroyed its internal structure.

3.2 Adsorption Characteristics of Coal With Different Deformation Degrees

Adsorption data for the 8 samples were obtained from the abovementioned gas adsorption experiment, that is, adsorption

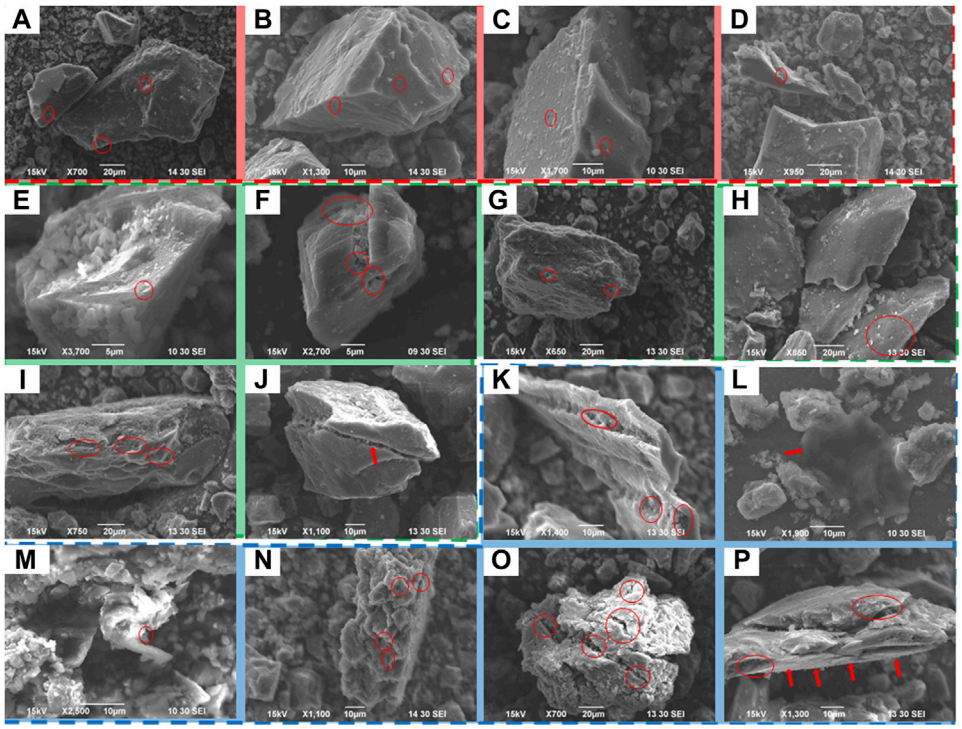

FIGURE 2 | SEM of images of **(A–D)** undeformed coal, **(E–J)** brittle deformed coal and **(K–P)** ductile deformed coal.

of CH_4 and CO_2 for coal size fractions of 0.12–0.15 mm, 0.18–0.25 and 0.42–0.84 mm. The results (on an air-dried basis) are presented in **Figure 3**.

CH_4 adsorption: The CH_4 adsorption results are shown in the three left-hand-side images of **Figure 3**, indicating that the adsorption capacity is lowest for undeformed coal and highest for high metamorphic grade and strong ductile deformed coal. The adsorption capacity of coal samples typically increases with the metamorphic grade (Yao and Liu, 2007; Zhang et al., 2009; Cai et al., 2013); however, **Figure 3** shows that the adsorption capacity of P02 ($R_{o,max}$ = 1.29%) is always lower than that of P01 ($R_{o,max}$ = 0.97%) and two of the brittle deformed coals (B01 and B02). The adsorption capacity increases with the metamorphic grade when the samples are classified as brittle and ductile deformed coal. The adsorption isotherms of brittle deformed sample B03 ($R_{o,max}$ = 1.31%) and ductile deformed sample D03 ($R_{o,max}$ = 1.93%) lie above those of B01 and B02 ($R_{o,max}$ = 1.08 and 1.11%, respectively) and D01 and D02 ($R_{o,max}$ = 1.57 and 1.63%, respectively). In addition, the fixed carbon content values of the samples of brittle deformed coal B01–03 and D01 are all between 60 and 62%, but their adsorption capacities vary greatly. The vitrinite content is lower in sample D03, which has the highest adsorption capacity (**Figure 3** and **Table 2**). The influence of carbon and vitrinite on the gas adsorption capacity of coal is affected by structural deformation according to **Figure 3** and **Table 2**. **Figure 3** also shows that the adsorption capacities of the three brittle deformed coals (B01–03) are larger than those of the high-rank weak ductile deformed coals (D01–D02) but smaller than that of the high-rank strong ductile deformed coal (D03). Thus, the deformation degree also affects the adsorption capacity.

CO_2 adsorption: The three images on the right-hand side of **Figure 3** show coal adsorption of CO_2, which is known to be much greater than that of CH_4 (Busch et al., 2003; Li et al., 2010; Han et al., 2013; Mustafa et al., 2020). Undeformed coal has the lowest adsorption capacity, whereas high metamorphic grade and strong ductile deformed coal have the highest adsorption capacity; the same general trends are observed for the CH_4 adsorption isotherms, although the details are different. The low adsorption capacities of the two high-rank weak ductile deformed coals for the 0.18–0.25 mm size fraction, samples D01 ($R_{o,max}$ = 1.56%) and D02 ($R_{o,max}$ = 1.63%), are even lower than that of sample P01 ($R_{o,max}$ = 0.97%), which has the lowest rank of the 8 samples (**Figure 3**). Thus, the adsorption capacity is also affected by the size fraction. Detailed results will be presented later.

The average Langmuir volumes for samples of the same type and size are plotted in **Figure 4**. Irrespective of the particle size and coal type, the Langmuir volume for CO_2 adsorption is always larger than that for CH_4 adsorption. For the same coal type, the sample with a 0.18–0.25 mm particle size has a larger Langmuir volume than the other particle size samples (0.12–0.15 and 0.42–0.84 mm). **Figure 4** also shows that the ductile deformed coal has the largest Langmuir volume of all the coal samples.

The adsorption capacities decrease in the following order: strong ductile deformed coal > brittle deformed coal > weak

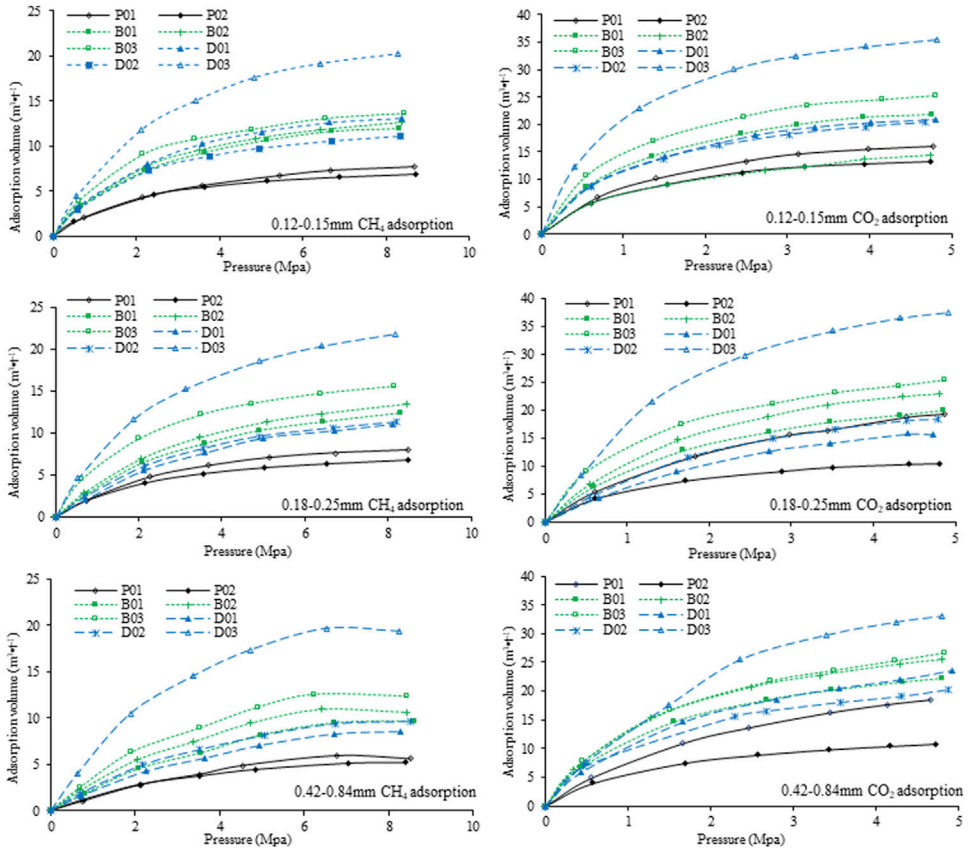

FIGURE 3 | CH_4 and CO_2 adsorption isotherms for coal samples with different size fractions.

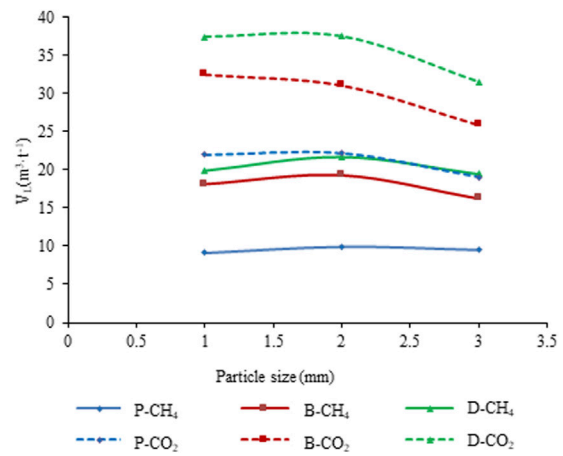

FIGURE 4 | Langmuir volume of undeformed coal and deformed coal samples with different size fractions.

ductile deformed coal > undeformed coal. **Figure 3** shows that the adsorption capacities of the three types of coal samples depend on the coal type, metamorphic grade, deformation process, adsorbed gas and size fraction.

3.3 Adsorption Characteristics of Coal With Different Particle Sizes

Undeformed coal (**Figure 5**): For CH_4 adsorption, the sample with the largest particles (0.42–0.84 mm) has a smaller adsorption capacity than those with other particle sizes (0.18–0.25 and 0.12–0.15 mm); that is, the adsorption capacities increase as the size fraction decreases. The coal samples with three particle sizes have similar CO_2 adsorption capacities in P01. The CO_2 adsorption isotherms of the 0.18–0.25 and 0.42–0.84 mm samples are similar in P02 and smaller than that of the smallest particle (0.12–0.15 mm) sample.

Brittle deformed coal (**Figure 5**): The CH_4 adsorption capacity of the 0.42–0.84 mm sample is always the smallest among the three particle size samples. The adsorption isotherms of the 0.18–0.25 mm coal sample are close for the 0.12–0.15 mm samples (B01 and B02), whereas that of B03 is slightly higher. The CO_2 adsorption isotherms for samples B01 and B03 with different size fractions of coal overlap; that is, there is little change in the adsorption capacity as the size fraction increases. However, the adsorption capacity slightly decreases as the size fraction decreases in sample B2.

Ductile deformed coal (**Figure 5**): The CH_4 adsorption curves of samples of 0.42–0.84 mm are basically at the lowest level, which are greatly different from the adsorption curves of samples of

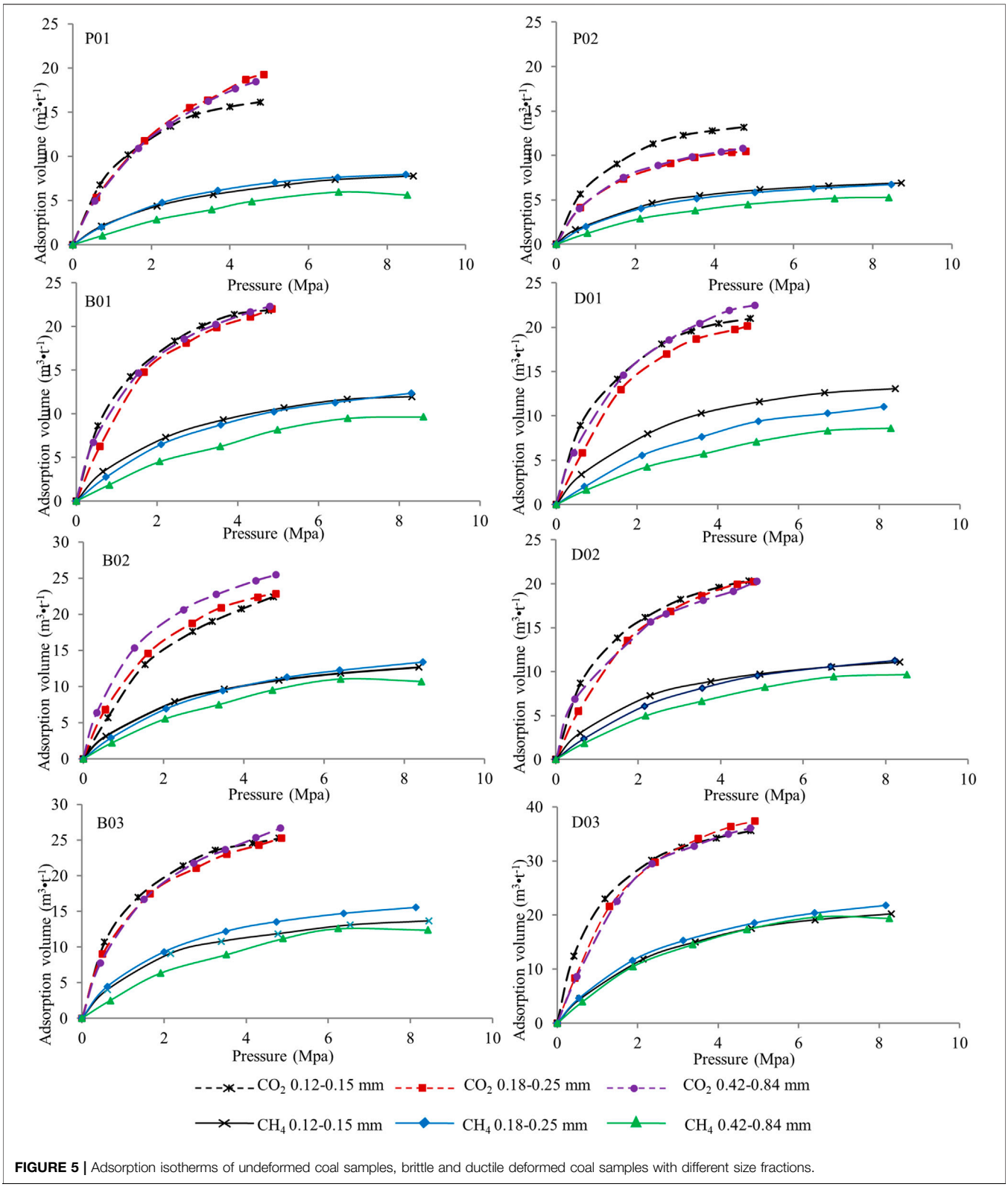

FIGURE 5 | Adsorption isotherms of undeformed coal samples, brittle and ductile deformed coal samples with different size fractions.

0.18–0.25 and 0.12–0.15 mm. The adsorption curve of the 0.18–0.25 mm sample is basically greater than or similar to that of the 0.12–0.15 mm sample. The stronger the deformation is, the closer the adsorption curves of the two particle sizes are, indicating that the deformation increases the number of pores and adsorption sites of the samples to some

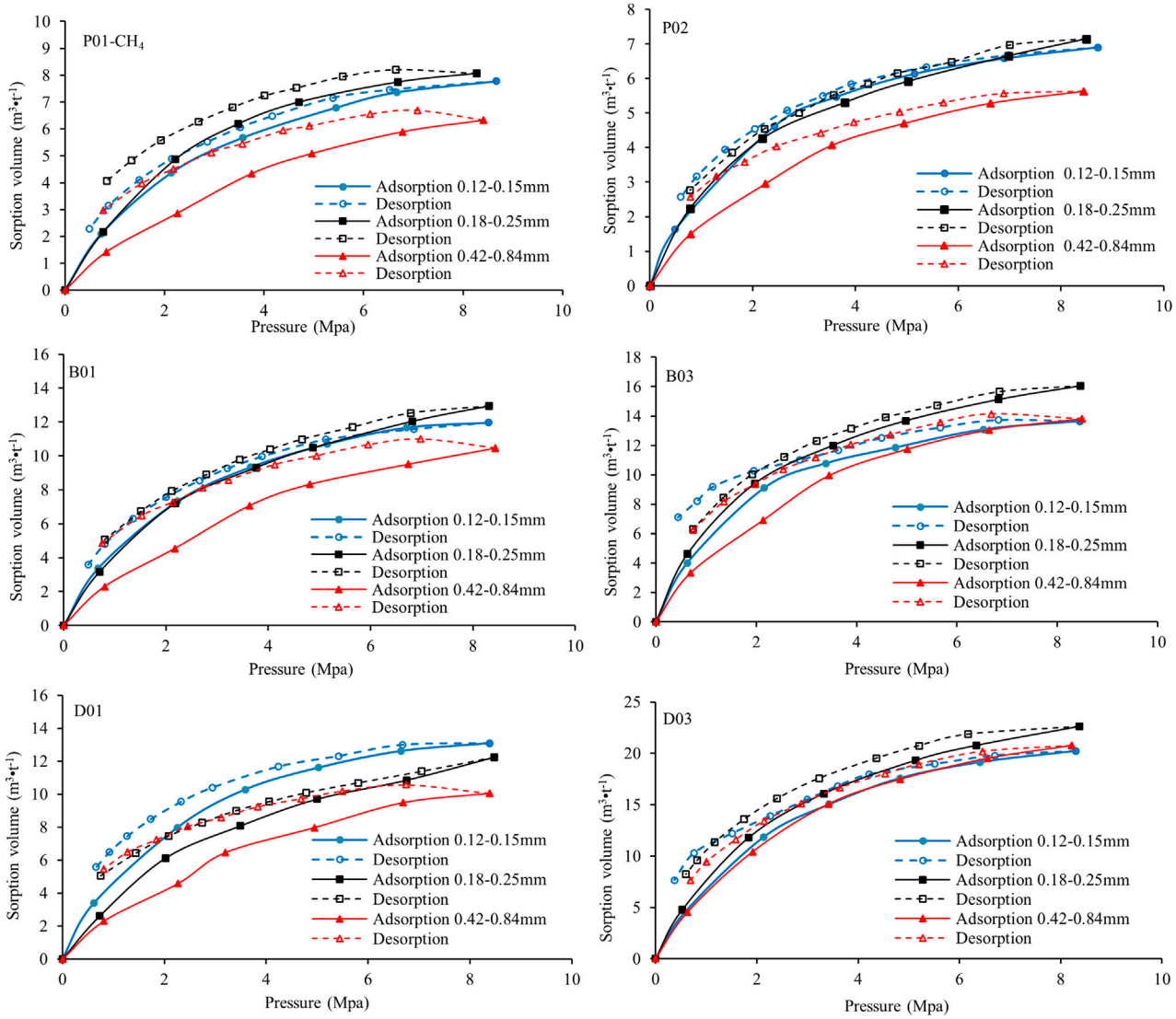

FIGURE 6 | CH_4 adsorption/desorption isotherms of coal samples with different size fractions.

extent, decreasing the influence of particle size on adsorption. The CO_2 adsorption isotherms of the three size fractions are similar, which means that the coal size fraction has little effect on the CO_2 adsorption capacity of brittle deformed coal.

Figure 5 also show that the coal adsorption capacity is much higher for CO_2 than for CH_4 at the same pressure. The coal size fraction affects the adsorption capacity for CH_4 for all 8 samples; that is, the adsorption capacity increases as the size fraction decreases from 0.42–0.84 to 0.18–0.25 mm. However, no obvious rule was found for the change in adsorption capacity from the 0.18–0.25 to 0.12–0.15 mm samples. The coal size fraction has a slightly smaller influence on CO_2 adsorption than on CH_4 adsorption. Moreover, deformation appears to reduce the effect of particle size on the adsorption capacity, especially in ductile deformed coal.

3.4 Desorption Characteristics of Deformed Coal Samples With Different Particle Sizes

CH_4 and CO_2 desorption isotherms were routinely measured after conducting the adsorption experiments (**Figures 6**, **7**). All previous adsorption/desorption studies have shown that the desorption isotherm generally lies above the adsorption isotherm (Han et al., 2013; Romanov et al., 2013; Shi et al., 2020). This hysteresis effect indicates that the sorbent/sorbate system is in a metastable state and that decreasing the pressure does not readily release the gas to an extent corresponding to the thermodynamic equilibrium value (Busch et al., 2003). **Figures 6**, **7** show hysteresis curves of various shapes for CH_4 and CO_2 for the deformed sample set with different size fractions.

For CH_4 (**Figure 6**), the 0.18–0.25 mm deformed coal samples exhibit the smallest deviations between the adsorption/desorption curves (little hysteresis), and all the samples release CH_4 in the first

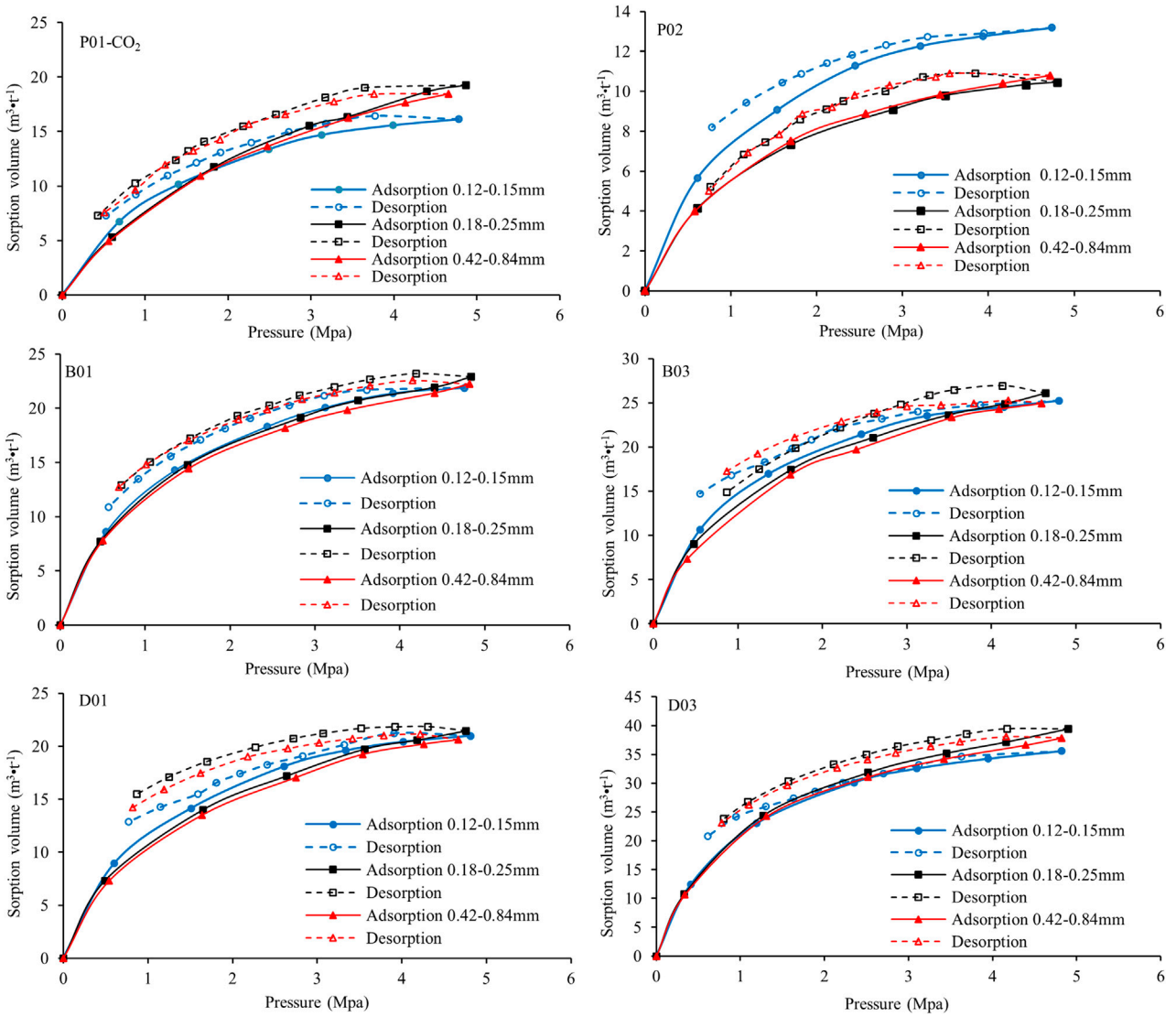

FIGURE 7 | CO_2 adsorption/desorption isotherms of coal samples with different size fractions.

TABLE 3 | Pore structure parameters obtained from CO_2 adsorption experiments on coal with different size fractions.

	0.42–0.84 (mm)			0.18–0.25 (mm)			0.12–0.15 (mm)		
	V **(cc/g)**	***S*** **(m^2/g)**	***w*** **(nm)**	***V*** **(cc/g)**	***S*** **(m^2/g)**	***w*** **(nm)**	***V*** **(cc/g)**	***S*** **(m^2/g)**	***w*** **(nm)**
P01	0.015	36.89	0.82	0.019	51.71	0.55	0.026	78.74	0.50
P02	0.017	45.80	0.82	0.022	60.25	0.52	0.034	101.51	0.50
B01	0.012	32.44	0.82	0.028	71.08	0.80	0.031	92.60	0.50
B02	0.023	62.97	0.8	0.037	99.71	0.62	0.040	122.17	0.50
B03	0.010	26.76	0.80	0.028	80.69	0.52	0.027	76.75	0.62
D01	0.011	25.26	0.82	0.019	51.35	0.82	0.018	48.27	0.52
D02	0.016	41.10	0.82	0.220	59.71	0.52	0.025	73.26	0.50
D03	0.051	152.76	0.50	0.040	130.4	0.50	0.060	196.0	0.48

desorption step. However, the 0.42–0.84 mm deformed coal samples, with the exception of D03, exhibit strong hysteresis, and mass balance shows a slight increase in the excess sorption. Andreas et al. explained this effect in terms of small inaccuracies in the experimental values, but changes in the coal volume from compressibility or swelling are also a possible cause (Busch et al., 2003). Thus, small deformed coal

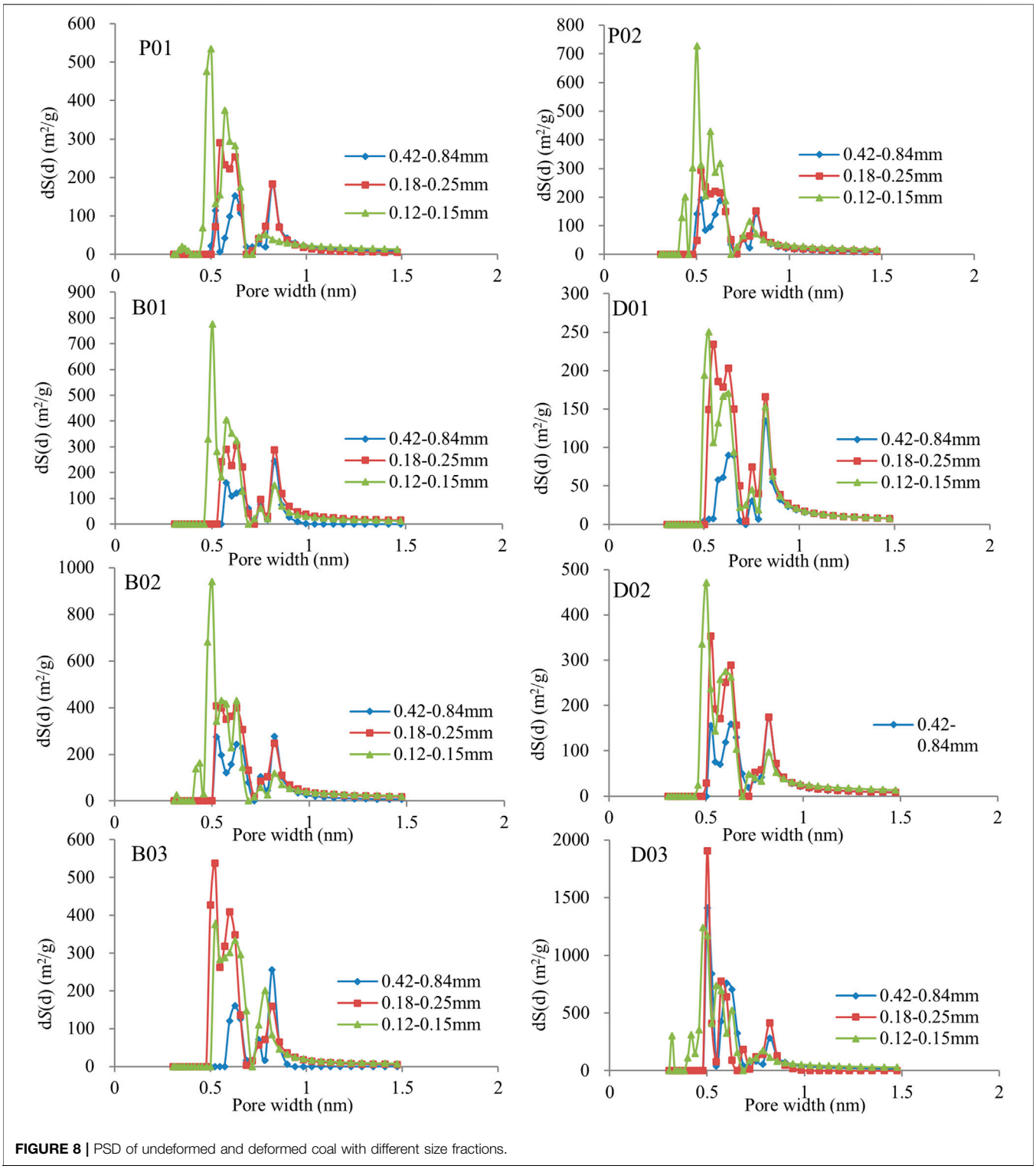

FIGURE 8 | PSD of undeformed and deformed coal with different size fractions.

particles can release CH_4 more easily than correspondingly larger particles. The desorption capacity of large coal particles increases under deformation.

For CO_2 (**Figure 7**), the deformed coal samples of all size fractions exhibit similarly strong hysteresis, especially sample D01, whereas sample D03 exhibits the least hysteresis. There is a small increase in the excess sorption in the first desorption step for all the samples. No change is observed in the desorption isotherms of the two undeformed coal samples with different size fractions when metamorphism increases. The hysteresis of the

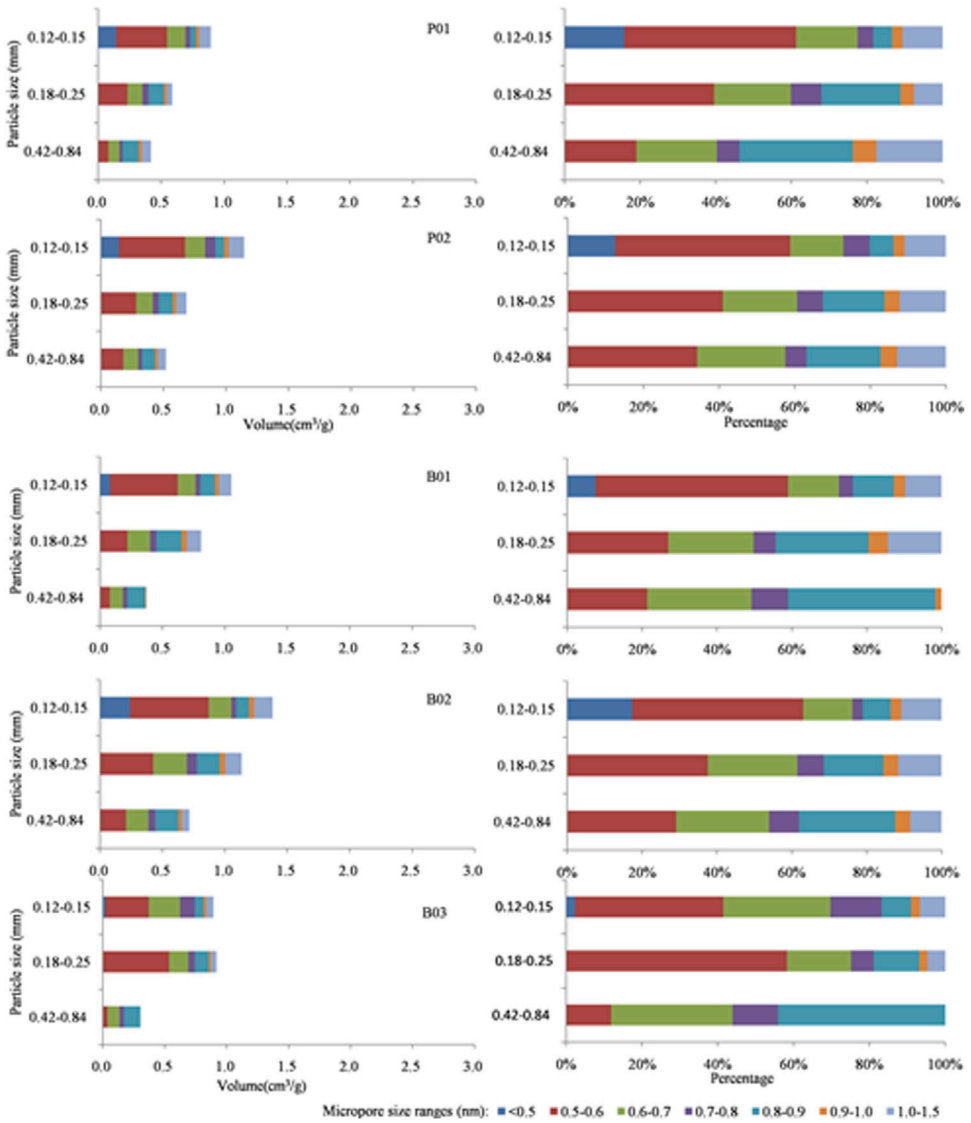

FIGURE 9 | Horizontal and stacked bar charts of undeformed coal and brittle deformed coal showing changes in the specific volume of micropore size ranges.

brittle and ductile deformed coals decreases as the deformation increases; that is, deformation promotes CO_2 desorption. For the same size fraction, there is stronger hysteresis for CO_2 than CH_4. The size fraction of the deformed coal samples clearly has no effect on the CO_2 desorption capacity, and CH_4 is more easily released than CO_2 in samples with the same size fraction. Furthermore, the higher desorption capacity of CH_4 relative to CO_2 decreases under deformation. That is, the effect of the size fraction on the gas desorption capacity of deformed coal is weakened by deformation.

3.5 Pore Size Distribution of Deformed Coal Samples With Different Particle Sizes

We compared the size distribution and parameters of coal pores for samples with different particle sizes, as obtained from a low-pressure CO_2 experiment. **Table 3** shows the pore structure parameters of coal with different size fractions, and **Figure 8** show the pore size distribution (PSD) of undeformed coal and deformed coal with different size fractions.

Figure 8 shows the PSD of undeformed coal for three size fractions. As the particle size decreases, the pore diameter decreases, and the specific surface area of the pores increases. The PSD of deformed coal for three size fractions can be described as follows (**Figure 8**): for weak brittle deformed coal (B1 and B2), as the particle size decreases, the pore specific surface area increases. However, in strong brittle deformed coal (B3), decreasing the particle size from 0.42–0.84 to 0.18–0.25 mm reduces the pore size and increases the pore specific surface area. Further decreases in the particle size (from 0.18–0.25 to 0.12–0.15 mm) do not affect the pores, and the pore specific surface area begins to decrease. In ductile deformed coal, similar

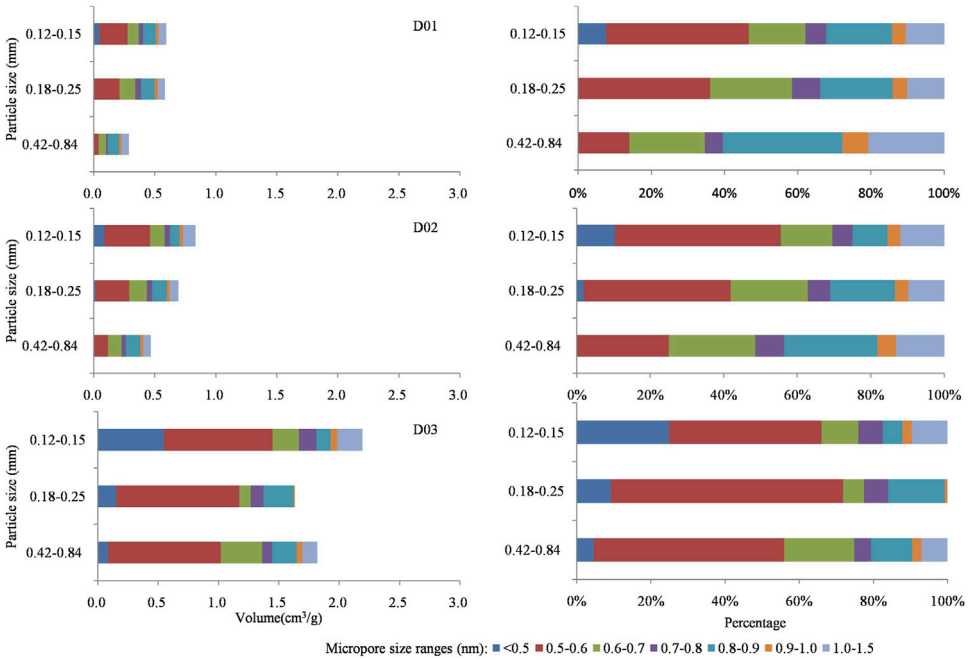

FIGURE 10 | Horizontal and stacked bar charts of ductile deformed coal showing changes in the specific volume of micropore size ranges.

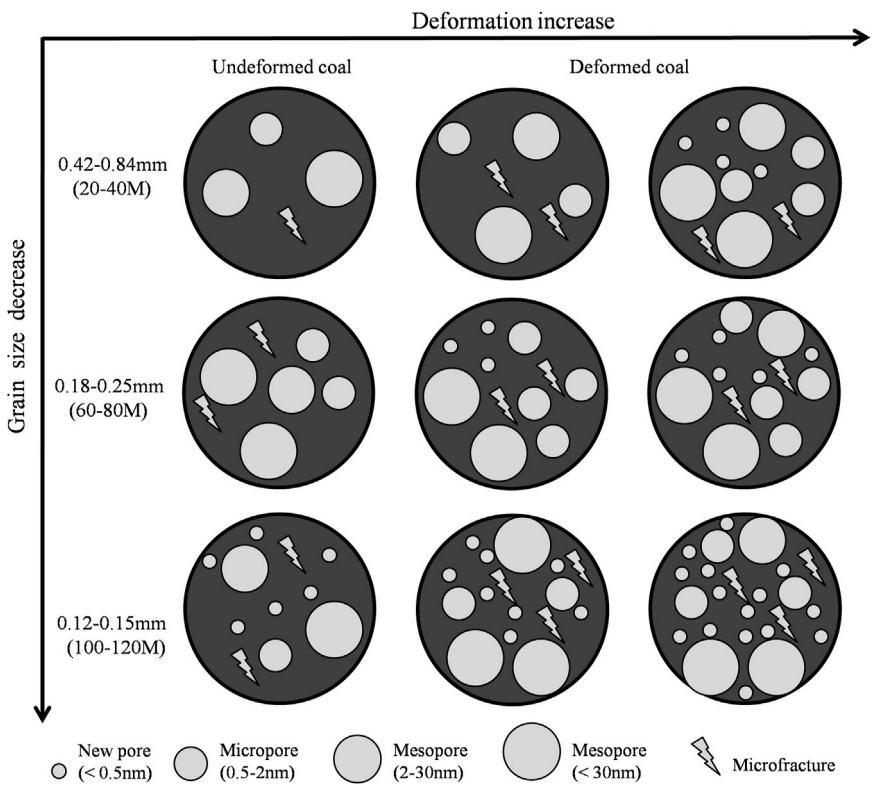

FIGURE 11 | Schematic drawings of pore structure changes of coal with grain size and deformation degree (Part of data support from Jia et al., 2013; Mastalerz et al., 2017).

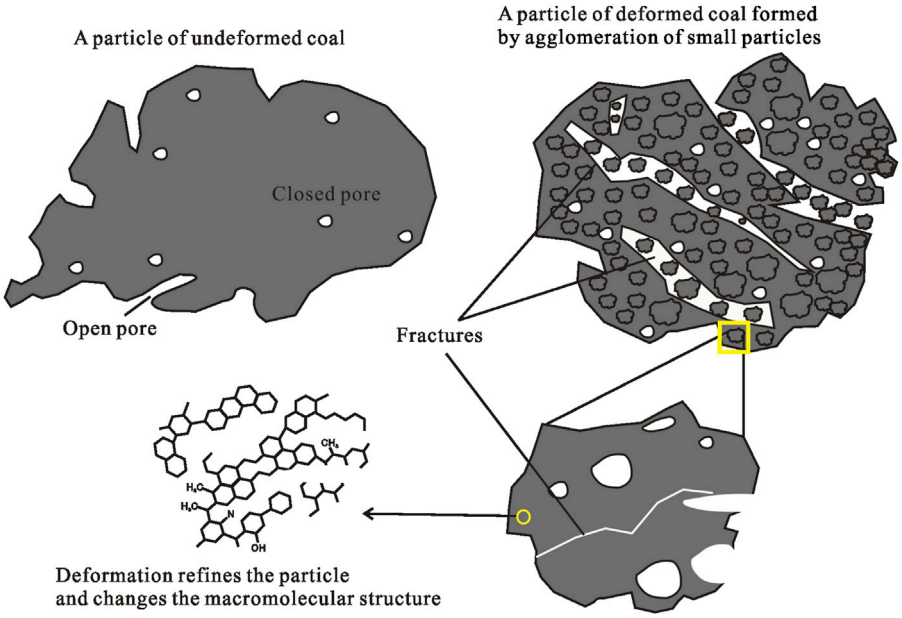

FIGURE 12 | Schematic diagram of characteristics of undeformed and deformed coal particles.

changes are observed under weak deformation (D1 and D2) and strong brittle deformation. Under strong ductile deformation (D3), as the particle size decreases, the pore specific surface area increases.

The PSD characteristics showed good consistency with the adsorption capacity. When the adsorption gas is CH_4, irrespective of the coal type, the largest sample size (0.42–0.84 mm) has the minimum pore specific surface area and adsorption/desorption volume (**Table 3**; **Figure 5**). Opposite trends are observed for the adsorption/desorption volume and the specific surface area for the other particle sizes (0.18–0.25 and 0.12–0.15 mm); that is, smaller particles lead to a smaller pore diameter and adsorption/desorption volume and a larger specific surface area. The smaller influence of the grain size on CO_2 adsorption than on CH_4 adsorption results from better penetration of the multisize pore structure of coal by CO_2 (Mastalerz et al., 2017), with CO_2 being smaller than CH_4 (kinetic diameters of CO_2 and CH_4 are 0.33 and 0.38 nm, respectively), and the influence of particle size on large pores is much stronger.

4 DISCUSSION

As the grain size of undeformed coal decreases, the abundance of 0.5–0.6 nm pores increase. However, a new pore size is added (<0.5 nm) when the grain size is 0.12–0.15 mm, and the pore sizes of other sizes are basically unchanged (**Figures 9**, **10**). Except for the D3 sample always having pores <0.5 nm, the other deformed coal samples obviously have new pores (<0.5 nm and 1.0–1.5 nm pores) as grinding proceeds. Therefore, the smaller the particle size is, the larger the pore volume in deformed coal samples. Pores <0.5 nm are developed in D3 samples regardless of particle size, while pores <0.5 nm appear in other samples only when the particle size reaches 0.12–0.15 mm. **Figure 11** shows the changes in pore structure with grain size and deformation degree. As the particle size of undeformed coal decreases, the abundance of pores larger than 30 nm increases, and that of 2–30 nm pores decrease (Jia et al., 2013; Mastalerz et al., 2017). However, the content of pores of different sizes was reported to increase in deformed coal as the particle size decreased (Fan et al., 2013; Li, et al., 2014; Wang et al., 2021). Thus, strong structural deformation can replace grinding action to impart coal with smaller pores and more pore types with different pore sizes (**Figure 11**).

If the sample collected includes deformed coal, the grain refinement caused by structural deformation must be considered in the sample preparation process. According to our experimental data, considering that the adsorption/desorption effects of the 0.12–0.15 and 0.18–0.25 mm samples are similar, the particle size of 0.12–0.15 mm can ensure that all deformed coal samples have more diverse pore sizes and reduce the influence of structural deformation on particle size (**Figure 11**). Therefore, if the adsorption/desorption characteristics of coal are studied from the perspective of structural deformation, it is recommended that the samples be crushed to 0.18–0.25 mm (60–80 mesh) to achieve the ideal adsorption/desorption effect without eliminating the influence of structural deformation. If the influence of structural deformation is not taken into account but the sample contains deformed coal (due to the extensive development of deformed coal in China), it is recommended that the sample be crushed below 0.12–0.15 mm (100–120 mesh) to reduce the impact of structural deformation on data processing and analysis (**Figure 11**).

The results and discussion above show that coal with different deformations exhibits significantly different adsorption/desorption curves and pore structure characteristics for the same particle size. However, for the same deformation type, the adsorption/desorption curves and pore structure characteristics of samples with different particle sizes can be similar. Thus, deformation has a stronger influence on the adsorption/desorption performance and internal structure of coal than granularity. The stronger the deformation is, the smaller the impact of the particle size on the adsorption/desorption properties of coal. This result is obtained because deformation changes both the internal structure and the macromolecular structure of coal (Qu, 2011; Li et al., 2013, 2017; Ju et al., 2018; Yang et al., 2020). Coal adsorption/desorption is closely related to coal pores, and the adsorption capacity is positively correlated with the total pore volume and the total pore specific surface area (Yao and Liu, 2007; Hou et al., 2017; Mastalerz et al., 2017; Pan et al., 2019). Structural deformation and sample granularity affect these parameters because the coal particle size is reduced by mechanical friction during deformation. The undeformed coal particles are intact, a few pores on the surface are connected to the outside, and the internal pores are still closed. However, the deformed coal particles are formed by agglomeration of smaller particles with more fractures distributed and more pores connected to the outside (**Figure 12**). The pore volume and the specific surface area vary with the coal particle size, which changes the total number of adsorption sites. Studies have shown that structural deformation can decrease the number of side chain functional groups of coal macromolecular structures while increasing the content of benzene ring structures and aromatic lamellar structures. Both the benzene ring structure and the lamellar gap can increase the gas adsorption/desorption potential and the gas adsorption capacity (Cao et al., 2003b; Ju and Li, 2009; Zhou 2010; Li et al., 2014; Yang et al., 2020). Therefore, structural deformation can also change the adsorption/desorption properties of coal *via* the macromolecular structure, which does not only depend on simple granularity factors.

5 CONCLUSION

1) Structural deformation has a great effect on the coal particles and internal structure, causes the granulation of coal and destroys its internal structure. The deformed coal particles and internal structure are formed by agglomeration of smaller particles with more fractures distributed and more pores connected to the outside. This means that deformed coal can provide more adsorption sites and adsorption space.
2) The adsorption capacity is always larger and faster for CO_2 than for CH_4 under the same pressure in deformed and undeformed coal. The adsorption capacities for CH_4 and CO_2 decrease in the following order: strong ductile deformed coal > brittle deformed coal > weak ductile deformed coal > undeformed coal.
3) A larger influence of the grain size and internal structure is observed on the adsorption/desorption of CH_4 than that of CO_2. Deformation affects the adsorption/desorption performance and the coal pore structure more strongly than granularity. The stronger the deformation is, the smaller the effect of the particle size and internal structure on coal adsorption/desorption. This relationship indicates that strong structural deformation can replace grinding action to impart coal with smaller pores and more pore types with different pore sizes.
4) The optimal size and internal structure during the adsorption experiment of deformed coal has been established, which can produce good-quality adsorption data of deformed coal for comparison with results from different studies. Our results demonstrate that the 0.18–0.25 mm (60–80 mesh) fraction for coal appears to be optimal and the most practical size range and internal structure for performing adsorption analysis if it is necessary to consider the influence of structural deformation. If the influence of structural deformation is not considered but the sample contains deformed coal (due to the extensive development of deformed coal in China), it is recommended that the sample be crushed below a smaller granularity (0.12–0.15 mm) to reduce the impact of structural deformation on data processing and analysis.

DATA AVAILABILITY STATEMENT

The original contributions presented in the study are included in the article/supplementary files, further inquiries can be directed to the corresponding author.

AUTHOR CONTRIBUTIONS

XL: Conceptualization, Data curation, Formal analysis, Writing-Original draft preparation. Visualization, Writing—review and editing. YJ: Writing—review and editing, Funding acquisition, Project administration. YS: Writing—review and editing. ZY: Resources, Investigation. QL: Resources, Investigation.

FUNDING

This work was supported by the National Natural Science Foundation of China (Grant Nos. 41672201, 41530315, 40972131, 41202120).

REFERENCES

Busch, A., Gensterblum, Y., and Krooss, B. M. (2003). Methane and CO2 Sorption and Desorption Measurements on Dry Argonne Premium Coals: Pure Components and Mixtures. *Int. J. Coal Geol.* 55, 205–224. doi:10.1016/s0166-5162(03)00113-7

Cai, Y., Liu, D., Pan, Z., Yao, Y., Li, J., and Qiu, Y. (2013). Pore Structure and its Impact on CH4 Adsorption Capacity and Flow Capability of Bituminous and Subbituminous Coals from Northeast China. *Fuel* 103, 258–268. doi:10.1016/j.fuel.2012.06.055

Cao, D. Y., and Zhang, S. R. (2003a). Deformation-metamorphic Types of High-Rank Coal in Northern Slope of the Dabie Mountains, Central China. *Sci. Geol. Sin.* 38 (4), 470–477. doi:10.3321/j.issn:0563-5020.2003.04.006

Cao, T., Song, Z., Wang, S., Cao, X., Li, Y., and Xia, J. (2015). Characterizing the Pore Structure in the Silurian and Permian Shales of the Sichuan Basin, China. *Mar. Petroleum Geol.* 61, 140–150. doi:10.1016/j.marpetgeo.2014.12.007

Cao, Y., Davis, A., Liu, R., Liu, X., and Zhang, Y. (2003b). The Influence of Tectonic Deformation on Some Geochemical Properties of Coals-A Possible Indicator of Outburst Potential. *Int. J. Coal Geol.* 53, 69–79. doi:10.1016/s0166-5162(02)00077-0

Castro-Marcano, F., Lobodin, V. V., Rodgers, R. P., McKenna, A. M., Marshall, A. G., and Mathews, J. P. (2012). A Molecular Model for Illinois No. 6 Argonne Premium Coal: Moving toward Capturing the Continuum Structure. *Fuel* 95 (0), 35–49. doi:10.1016/j.fuel.2011.12.026

Chen, Y., Wang, X., and He, R. (2011). Modeling Changes of Fractal Pore Structures in Coal Pyrolysis. *Fuel* 90 (2), 499–504. doi:10.1016/j.fuel.2010.10.016

Crosdale, P. J., and Beamish, B. B. (1993). *Beeston J W. New Developments in Coal Geology: A Symposium*. Brisbane: Geological Society of Australia, 95–98.Maceral Effects on Methane Sorption by Coal

Cui, Y. J., Li, Y. H., Zhang, Q., and Jiang, W. P. (2005). The Characteristic Curve of Coal Adsorption Methane and its Role in the Study of Coalbed Methane Reservoir. *Chin. Sci. Bull.* 50 (1), 76–81. doi:10.1007/bf03184088

Domazetis, G., Raoarun, M., James, B. D., and Liesegang, J. (2008). Molecular Modelling and Experimental Studies on Steam Gasification of Low-Rank Coals Catalysed by Iron Species. *Appl. Catal. A General.* 340 (1), 105–118. doi:10.1016/j.apcata.2008.01.037

Dyrkacz, G. R., and Horwitz, E. P. (1982). Separation of Coal Macerals. *Fuel* 61 (1), 3–12. doi:10.1016/0016-2361(82)90285-x

Fan, J. J., Ju, Y. W., Liu, S. B., and Li, X. S. (2013). Micropore Structure of Coals under Different Reservoir Conditions and its Implication for Coalbed Methane Development. *J. China Coal Soc.* 3 (38), 441–447.

Fengli, L., Bo, J., Guoxi, C., Yu, S., and Zheng, T. (2019a). Structural and Evolutionary Characteristics of Pores-Microfractures and Their Influence on Coalbed Methane Exploitation in High-Rank Brittle Tectonically Deformed Coals of the Yangquan Mining Area, Northeastern Qinshui Basin, China. *J. Petroleum Sci. Eng.* 174, 1290–1302. doi:10.1016/j.petrol.2018.11.081

Furmann, A., Mastalerz, M., Bish, D., Schimmelmann, A., and Pedersen, P. K. (2016). *Porosity and Pore-Size Distribution in Shales from the Belle Fourche and Second White Specks Formations in Alberta, Canada*. American Association of Petroleum Geologists.

Gayer, R., and Harris, I. (1996). *Coalbed Methane and Coal Geology*. London: London:The Geological Society, 1–338.

Gilfillan, A., Lester, E., Cloke, M., and Snape, C. (1999). The Structure and Reactivity of Density Separated Coal Fractions. *Fuel* 78 (14), 1639–1644. doi:10.1016/s0016-2361(99)00110-6

Guo, B. W. (2001). Geological Analysis on Relationship Between Structural Coal Characteristics and Carbon Dioxide Outburst. *Coal Geol. Explor.* 29 (1), 28–30. doi:10.3969/j.issn.1001-1986.2001.01.009

Han, F., Busch, A., Krooss, B. M., Liu, Z., and Yang, J. (2013). CH4 and CO2 Sorption Isotherms and Kinetics for Different Size Fractions of Two Coals. *Fuel* 108, 137–142. doi:10.1016/j.fuel.2011.12.014

Hou, Q. L., Li, P. J., and Li, J. L. (1995). *Foreland Fold-Thrust Belt in Southwestern Fujian*. Beijing, China: Geology Publishing House.

Hou, S., Wang, X., Wang, X., Yuan, Y., Pan, S., and Wang, X. (2017). Pore Structure Characterization of Low Volatile Bituminous Coals with Different Particle Size and Tectonic Deformation Using Low Pressure Gas Adsorption. *Int. J. Coal Geol.* 183, 1–13. doi:10.1016/j.coal.2017.09.013

Islam, M. R., and Hayashi, D. (2008). Geology and Coal Bed Methane Resource Potential of the Gondwana Barapukuria Coal Basin, Dinajpur, Bangladesh. *Int. J. Coal Geol.* 75 (3), 127–143. doi:10.1016/j.coal.2008.05.008

Jia, Y. N., Wen, Z. H., and Wei, J. P. (2013). Experimental Study on Gas Desorption Laws of Coal Samples with Different Particle Size. *Saf. Coal Mines* 07, 1–3.

Jiang, B., and Ju, Y. W. (2004). Tectonic Coal Structure and its Petrophysical Features. *Nat. Gas. Ind.* 24 (5), 27–29. doi:10.3321/j.issn:1000-0976.2004.05.009

Jiang, W. P., Zhang, Q. L., and Cui, Y. J. (2010). Mechanism Study on the Influence of CO_2 on CH_4 Adsorption on Different Rank Coals. *China Coalbed Methane* 4 (7), 19–22. doi:10.3969/j.issn.1672-3074.2010.04.005

Ju, Y., Jiang, B., and Hou, Q. L. (2005a). Relationship between Nanoscale Deformation of Coal Structure and Metamorphic-Deformed Environments. *Chin. Sci. Bull.* 50 (16), 1784–1795. doi:10.1360/04wd0205

Ju, Y., Jiang, B., Hou, Q., Wang, G., and Ni, S. (2005b). 13 C NMR Spectra of Tectonic Coals and the Effects of Stress on Structural Components. *Sci. China Ser. D-Earth Sci.* 48 (9), 1418–1437. doi:10.1360/04yd0199

Ju, Y., and Li, X. (2009). New Research Progress on the Ultrastructure of Tectonically Deformed Coals. *Prog. Nat. Sci.* 19, 1455–1466. doi:10.1016/j.pnsc.2009.03.013

Ju, Y., Sun, Y., Tan, J., Bu, H., Han, K., Li, X., et al. (2018). The Composition, Pore Structure Characterization and Deformation Mechanism of Coal-Bearing Shales from Tectonically Altered Coalfields in Eastern China. *Fuel* 234, 626–642. doi:10.1016/j.fuel.2018.06.116

Ju, Y. W., Jiang, B., Hou, Q. L., and Wang, G. L. (2004). The New Structure-Genetic Classification System in Tectonically Deformed Coals and its Geological Significance. *J. China Coal Soc.* 29 (5), 513–517. doi:10.3321/j.issn:0253-9993.2004.05.001

Laxminarayana, C., and Crosdale, P. J. (1999). Role of Coal Type and Rank on Methane Sorption Characteristics of Bowen Basin, Australia Coals. *Int. J. Coal Geol.* 40 (4), 309–325. doi:10.1016/s0166-5162(99)00005-1

Li, D., Liu, Q., Weniger, P., Gensterblum, Y., Busch, A., and Krooss, B. M. (2010). High-pressure Sorption Isotherms and Sorption Kinetics of CH4 and CO2 on Coals. *Fuel* 89, 569–580. doi:10.1016/j.fuel.2009.06.008

Li, X., Ju, Y., Hou, Q., Li, Z., Wei, M., and Fan, J. (2014). Characterization of Coal Porosity for Naturally Tectonically Stressed Coals in Huaibei Coal Field, China. *ScientificWorldJournal* 2014, 560450. doi:10.1155/2014/560450

Li, X., Ju, Y., Hou, Q., Li, Z., Li, Q., and Wang, G. (2017). Nanopore Structure Analysis of Deformed Coal from Nitrogen Isotherms and Synchrotron Small Angle X-Ray Scattering. *J. Nanosci. Nanotechnol.* 17 (9), 6224–6234. doi:10.1166/jnn.2017.14444

Li, X. S., Ju, Y. W., Hou, Q. L., and Fan, J. J. (2013). Response of Macromolecular Structure to Deformation in Tectonically Deformed Coal. *Acta Geol. sin.-engl.* 87 (1), 82–90. doi:10.1111/1755-6724.12032

Li, X. S., Ju, Y. W., Hou, Q. L., and Lin, H. (2012). Spectra Response from Macromolecular Structure Evolution of Tectonically Deformed Coal of Different Deformation Mechanisms. *Sci. China, Ser. D.* 55 (1), 1–11. doi:10.1007/s11430-012-4399-y

Li, Z., Liu, D., Cai, Y., Wang, Y., and Teng, J. (2019b). Adsorption Pore Structure and its Fractal Characteristics of Coals by N2 Adsorption/desorption and FESEM Image Analyses. *Fuel* 257 (1), 116031. doi:10.1016/j.fuel.2019.116031

Marcin, L., and Miguel Á., G. G. (2016). Characteristics of Carbon Dioxide Sorption in Coal and Gas Shale the Effect of Particle Size. *J. Nat. Gas Sci. Eng.* 28, 558–565. doi:10.1016/j.jngse.2015.12.037

Mastalerz, M., Hampton, L., Drobniak, A., and Loope, H. (2017). Significance of Analytical Particle Size in Low-Pressure N2 and CO2 Adsorption of Coal and Shale. *Int. J. Coal Geol.* 178, 122–131. doi:10.1016/j.coal.2017.05.003

Mathews, J. P., van Duin, A. C. T., and Chaffee, A. L. (2011). The Utility of Coal Molecular Models. *Fuel Process. Technol.* 92 (4), 718–728. doi:10.1016/j.fuproc.2010.05.037

Moore, T. A. (2012). Coalbed Methane: A Review. *Int. J. Coal Geol.* 101, 36–81. doi:10.1016/j.coal.2012.05.011

Mustafa, A., Suriati, S., Mohamad, A. B., Usama, E., Humbul, S., Roberto, B., et al. (2020). Experimental Measurements of Carbon Dioxide, Methane and Nitrogen High-Pressure Adsorption Properties onto Malaysian Coals under Various Conditions. *Energy* 210, 118575.

Pan, J., Hou, Q., Ju, Y., Bai, H., and Zhao, Y. (2012). Coalbed Methane Sorption Related to Coal Deformation Structures at Different Temperatures and Pressures. *Fuel* 102, 760–765. doi:10.1016/j.fuel.2012.07.023

Pan, J., Lv, M., Hou, Q., Han, Y., and Wang, K. (2019). Coal Microcrystalline Structural Changes Related to Methane Adsorption/desorption. *Fuel* 239, 13–23. doi:10.1016/j.fuel.2018.10.155

Qu, Z. H., Jiang, B., Wang, J. L., Dou, X. Z., and Li, M. (2012). Evolution of Textures and Stress-Strain Environments of Tectonically-Deformed Coals. *Geol. J. Chin. Univ.* 18 (3), 453–459. doi:10.16108/j.issn.1006-7493.2012.03.017

Qu, Z. H. (2011). Study of Tectonized Coal Texture and its Controlling Mechanism on Gas Properties. *J. China Coal Soc.* 3 (36), 533–534.

Romanov, V. N., Hur, T.-B., Fazio, J. J., Howard, B. H., and Irdi, G. A. (2013). Comparison of High-Pressure CO2 Sorption Isotherms on Central Appalachian and San Juan Basin Coals. *Int. J. Coal Geol.* 118, 89–94. doi:10.1016/j.coal.2013.05.006

Shi, F., Wei, Z., Zhang, D., and Huang, G. (2020). Isotherms and Kinetics of Deformation of Coal during Carbon Dioxide Sequestration and Their Relationship to Sorption. *Int. J. Coal Geol.* 231, 103606. doi:10.1016/j.coal.2020.103606

Sun, R. Y., Li, L., Wang, N., Zhang, Y., Hu, A., and Dong, C. (2012). Evaluation of Factors Influencing Adsorption Property of Coal and Rocks. *China Coalbed Methane* 2 (9), 10–12. doi:10.3969/j.issn.1672-3074.2012.02.003

Swanson, S. M., Mastalerz, M. D., Engle, M. A., Valentine, B. J., Warwick, P. D., Hackley, P. C., et al. (2015). Pore Characteristics of Wilcox Group Coal, U.S. Gulf Coast Region: Implications for the Occurrence of Coalbed Gas. *Int. J. Coal Geol.* 139, 80–94. doi:10.1016/j.coal.2014.07.012

Wang, E. Y., Liu, M. J., and Wei, J. P. (2009). New Genetic-Texture Structure Classification System of Tectonic Coal. *J. China Coal Soc.* 34 (5), 656–660.

Wang, G., and Ju, Y. (2015). Organic Shale Micropore and Mesopore Structure Characterization by Ultra-low Pressure N 2 Physisorption: Experimental Procedure and Interpretation Model. *J. Nat. Gas Sci. Eng.* 27, 452–465. doi:10.1016/j.jngse.2015.08.003

Wang, G. Y., Wu, G. G., and Li, Q. H. (2005). Coal Maceral Separation Technology and It's Application. *China coal.* 31 (8), 52–54. doi:10.19880/j.cnki.ccm.2005.08.021

Wang, X., Cheng, Y., Zhang, D., Liu, Z., Wang, Z., and Jiang, Z. (2021). Influence of Tectonic Evolution on Pore Structure and Fractal Characteristics of Coal by Low Pressure Gas Adsorption. *J. Nat. Gas Sci. Eng.* 87, 103788. doi:10.1016/j.jngse.2020.103788

Yang, Y., Pan, J., Wang, K., and Hou, Q. (2020). Macromolecular Structural Response of Wender Coal under Tensile Stress via Molecular Dynamics. *Fuel* 265, 116938. doi:10.1016/j.fuel.2019.116938

Yao, Y. B., and Liu, D. M. (2007). Adsorption Characteristics of Coal Reservoirs in North China and its Influencing Factors. *J. China Univ. Min. &Technol.* 3 (36), 308–314. doi:10.3321/j.issn:1000-1964.2007.03.007

Yu, H. G., Fan, W. T., Sun, M. Y., and Ye, J. P. (2004). Study on Fitting Models for Methane Isotherms Adsorption of Coals. *J. China Coal Soc.* 29 (4), 463–467. doi:10.3321/j.issn:0253-9993.2004.04.019

Zhang, T. J., Xu, H. J., Li, S. G., and Ren, S. X. (2009). The Effect of Particle Size on Adsorption of Methane on Coal. *J.Hunan Univ. Sci. Technol.* 1 (24), 9–12. doi:10.3969/j.issn.1672-9102.2009.01.003

Zhong, L. W., Zheng, Y. Z., Yun, Z. R., Lei, C. L., and Zhang, H. (2002). The Adsorption Capability of Coal under Integrated Influence of Temperature and Pressure and Predicted of Content Quantity of Coalbed Gas. *J. China Coal Soc.* 6 (27), 581–585. doi:10.3321/j.issn:0253-9993.2002.06.005

Zhou, J. P. (2010). Effect of Different Adsorptional Gases on Permeability of Coal. *Chin. J. Rock Mech. Eng.* 1 (29), 2256–2262.

Zhu, H., Ju, Y., Huang, C., Chen, F., Chen, B., and Yu, K. (2020). Microcosmic Gas Adsorption Mechanism on Clay-Organic Nanocomposites in a Marine Shale. *Energy* 197, 117256. doi:10.1016/j.energy.2020.117256

Zhu, H., Ju, Y., Qi, Y., HuangZhang, C. L., and Zhang, L. (2018). Impact of Tectonism on Pore Type and Pore Structure Evolution in Organic-Rich Shale: Implications for Gas Storage and Migration Pathways in Naturally Deformed Rocks. *Fuel* 228, 272–289. doi:10.1016/j.fuel.2018.04.137

Zou, J., and Rezaee, R. (2016). Effect of Particle Size on High-Pressure Methane Adsorption of Coal. *Petroleum Res.* 1 (1), 53–58. doi:10.1016/s2096-2495(17)30030-3

Conflict of Interest: The authors declare that the research was conducted in the absence of any commercial or financial relationships that could be construed as a potential conflict of interest.

Publisher's Note: All claims expressed in this article are solely those of the authors and do not necessarily represent those of their affiliated organizations, or those of the publisher, the editors and the reviewers. Any product that may be evaluated in this article, or claim that may be made by its manufacturer, is not guaranteed or endorsed by the publisher.